BIOCHEMISTRY, BIOPHYSICS, AND MOLECULAR BIOLOGY

Quantum-Classical Model of Retinal Photoisomerization Reaction in Visual Pigment Rhodopsin

V. D. Lakhno[a], **A. S. Shigaev**[a,*], **T. B. Feldman**[b,c], **V. A. Nadtochenko**[d], and Academician **M. A. Ostrovsky**[b,c]

Received August 17, 2016

Abstract—A quantum-classical model of photoisomerization of the visual pigment rhodopsin chromophore is proposed. At certain (and more realistic) parameter value combinations, the model is shown to accurately reproduce a number of independent experimental data on the photoreaction dynamics: the quantum yield, the time to reach the point of conical intersection of potential energy surfaces, the termination time of the evolution of quantum subsystem, as well as the characteristic low frequencies of retinal molecular lattice fluctuations during photoisomerization. In addition, the model behavior is in good accordance with experimental data about coherence and local character of quantum transition.

The visual pigment rhodopsin is a typical representative of the large family of G protein-coupled receptors, which play a key role in the regulatory processes in living organisms [1]. The rhodopsin molecule consists of the opsin protein and the 11-*cis* retinal chromophore, which is covalently linked to the protein moiety of the molecule through a protonated bond of the Schiff base with the amino group of lysine (Lys 296). The absorption of a light quantum leads to the isomerization of 11-*cis* retinal into the *trans*-form, which, in turn, alters the conformation of the protein moiety of the molecule and eventually triggers the transduction process.

The photoisomerization of 11-*cis* retinal is the first and the only photochemical reaction in visual perception. This reaction is one of the fastest in nature. The elementary act of the chromophore photoisomerization in rhodopsin continues for approximately 80−100 fs [2, 3] with a quantum yield of 0.67 [4], and the formation of the primary photoproduct in the ground state is completed within 200 fs [5]. It should be noted that oscillations in the kinetic absorption curves of the

reaction products are observed, which are due to the formation of coherent vibrational wave packets [2, 3, 5].

The conventional model of rhodopsin photoisomerization is shown in Fig. 1. The elementary primary act of retinal isomerization into rhodopsin is interpreted as a non-activated passage of a conical intersection between the potential energy surfaces (PES) of the electronically excited state S_1 and the ground state of products S_0.

The majority of researchers believe that the photoisomerization of 11-*cis*-retinal in rhodopsin is associated with a strictly local shift of its atomic groups in the area of the double bond $C_{11} = C_{12}$ [3, 6]. This assumption is indirectly confirmed by the data on a strong electrostatic interaction between the β-ionone ring of retinal with the amino acid residues of opsin [7, 8]. Indeed, the rigid fixation of 11-*cis* retinal in the β-ionone ring and the impossibility of free rotation around the $C_7 = C_8$ bond greatly limit the area of conformational changes of the chromophore during its photoisomerization. The elementary and local nature of the act of photoisomerization of the rhodopsin chromophore makes it possible to study its mechanism by using simple mathematical models.

This paper presents the results of the study of photoisomerization of 11-*cis*-retinal in rhodopsin using a simple quantum-classical model. A similar approach has worked well earlier in the theoretical study of the primary charge separation in the reaction center of bacteria [9, 10] and the electric charge migration in DNA [11].

The model comprises two subsystems. The quantum subsystem consists of three states: S_{0Rh}—rhodopsin molecule in the ground state, corresponding to Rh_{498} in Fig. 1; S_{1Rh}—photoexcited state; S_{0Photo}—pri-

[a]*Institute of Mathematical Problems of Biology, Russian Academy of Sciences—branch of Keldysh Institute of Applied Mathematics, Russian Academy of Sciences, Pushchino, Moscow oblast, 142290 Russia*
[b]*Moscow State University, Moscow, 119991 Russia*
[c]*Emanuel Institute of Biochemical Physics, Russian Academy of Sciences, Moscow, 117977 Russia*
[d]*Semenov Institute of Chemical Physics, Russian Academy of Sciences, Moscow, 119991 Russia*
[*]*e-mail: shials@rambler.ru*
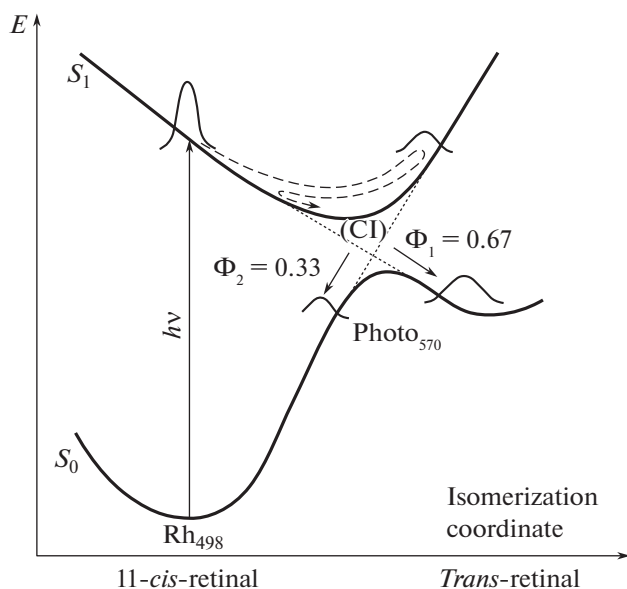
Fig. 1. Scheme of the PES reaction of rhodopsin photoisomerization. The absorption of a light quantum leads to the transition from the dark rhodopsin Rh_{498} from the ground S_0 level of PES to the excited level S_1. Then, the reaction coordinate reaches the conical intersection (CI) with subsequent transition to one of the ground states: the primary photoproduct $Photo_{570}$ or the original rhodopsin Rh_{498} with 11-*cis*-retinal.

mary photoproduct containing *trans*-retinal. The wave functions of the states S_{0Rh}, S_{1Rh}, and S_{0Photo} are described by variables b_0, b_1, and b_X, respectively. By the condition of normalization, the sum of the squares of their absolute values is equal to unity. S_{0Rh}, S_{1Rh}, and S_{0Photo} energies are set through diagonal matrix elements ν_0 (corresponds to the Rh_{498} minimum in Fig. 1), ν_1 (excited state), and ν_X (minimum $Photo_{570}$ in Fig. 1). For simplicity, $\nu_1 = 0$ and, consequently, ν_0 (S_{0Rh}) $< \nu_X$ (S_{0Photo}) < 0.

The classical system is represented by two effective point masses M_1 and M_X, which simulate the arbitrary parts of the chromophore that change their position during photoisomerization. The coordinates of the point masses are described by variables $?_1$ and $?_X$, and the degree of their shift is regulated by elastic constants K_1 and K_X. The motion of the model is described by the following equations:

$$\hbar i \frac{db_0}{d\tilde{t}} = \nu_{01}b_1 + \nu_{0X}b_X + \nu_0 b_0,$$

$$\hbar i \frac{db_1}{d\tilde{t}} = \nu_{1X}b_X + \nu_{01}b_0 + \alpha' \tilde{u}_1 b_1,$$

$$\hbar i \frac{db_X}{d\tilde{t}} = \nu_{1X}b_1 + \nu_{0X}b_0 + \alpha' \tilde{u}_X b_X + \nu_X b_X, \quad (1)$$

$$M_1 \frac{d^2 \tilde{u}_1}{d\tilde{t}^2} = -K_1 \tilde{u}_1 - \gamma \frac{d\tilde{u}_1}{d\tilde{t}} - \alpha' |b_1|^2,$$

$$M_X \frac{d^2 \tilde{u}_X}{d\tilde{t}^2} = -K_X \tilde{u}_X - \gamma \frac{d\tilde{u}_X}{d\tilde{t}} - \alpha' |b_X|^2,$$

where α' is the constant of the coupling of the quantum subsystems with the classical one; ν_{01}, ν_{0X}, and ν_{1X} are the non-diagonal matrix elements of the transition between the quantum subsystem states; and γ is the friction coefficient.

On the basis of the wavelengths absorbed by states Rh_{498} (S_{0Rh}) and $Photo_{570}$ (S_{0Photo}) (500 and 570 nm, respectively), it can be easily found that $\nu_0 = -2.481$ eV and $\nu_X = -2.17$ eV. However, for the non-diagonal matrix elements ν_{01}, ν_{0X}, and ν_{1X}, even their approximate values can hardly be estimated. For this reason, these parameters varied within a broad range. For the coupling constant α', only the maximum value from the energy and length of the $C_{11} = C_{12}$ bond can be calculated. Knowing the $C = C$ bond energy (approximately 6.5 eV) and taking its effective length as 1 Å (the real length is 1.34 Å), we approximately obtain the condition $\alpha' \leq 6.5$ eV $\cdot$ Å^{-1}. Thus, the quantum subsystem contains four variable parameters: ν_{01}, ν_{0X}, ν_{1X}, and α'.

The parameters of the classical subsystem were evaluated on the basis of general considerations of molecular biophysics. As discussed above, one of the boundaries of the area of conformational changes during 11-*cis*-retinal photoisomerization is, obviously, the C_8 atom of the polyenoic chain. On the other hand, according to the published data, the methyl group of the C_{20} atom is also actively involved in this reaction [12]. Therefore, the point masses of the model M_1 and M_X must be located in the chromophore region from C_8 to C_{15} (Fig. 2).

We assumed that M_1 corresponds to the sum of masses of the methyl group C_{20} and C_{13} atom, and M_X corresponds to the sum of masses of the C_9 atom and the methyl group C_{19}: $M_1 = M_X = 27$ amu. Due to the homogeneity of the conjugated bonds of the polyenoic chain, the elastic constants K_1 and K_X are also taken to be equal: $K_1 = K_X = K$.

The range of K values was estimated from the experimental data [13]. According to these data, the main vibrational modes involved in the chromophore photoisomerization lie in the range from 969 to 1548 cm^{-1}. Designate ν the corresponding frequencies in dimension [s^{-1}] and select the characteristic time $\tau = 10^{-15}$ s. As a result, the elastic constant can be expressed through the dimensionless frequency square ω^2 for convenience of further calculations:

$$\omega^2 = \frac{K\tau^2}{M} = \nu^2 \tau^2. \quad (2)$$

For the above-mentioned range ν, we obtain $0.000845 \leq \omega^2 \leq 0.00213$. The actual working range of ω^2, used in the calculations, was 0.0005–0.003. The
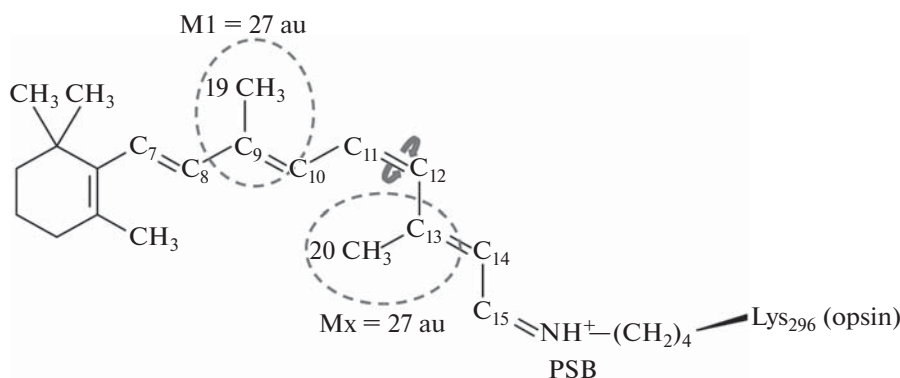
Fig. 2. The structure of 11-*cis*-retinal, which is covalently bound to the lysine residue (Lys 296) of opsin through the Schiff base bond (PSB). The nuclear groups marked with the oval correspond to the effective point masses M_1 and M_X, equal to 27 au. The round arrows in the $C_{11} = C_{12}$ bond region designate the site of photoisomerization of 11-*cis*-retinal into the *trans*-form.

usual value for the quantum−classical models of DNA 0.6×10^{-12} H m^{-1} s [11] was taken as the basis of the coefficient γ. With allowance for the high viscosity within the protein globule, the value of this coefficient was taken 2.5 times higher: $\gamma = 1.5 \times 10^{-12}$ H m^{-1} s.

By introducing, in addition to ω^2 and τ, the characteristic shift value U, require implementation of the relation linking the scale of the shift of point masses with the bound constant α':

$$\alpha'\tau^2/(MU) = 1. \qquad (3)$$

As a result, all values of the model can be expressed through the dimensionless equivalents:

$$t = \frac{\tilde{t}}{\tau}, \quad u_n = \frac{\tilde{u}_n}{U}, \quad \Omega = \frac{\gamma \cdot \tau}{M}, \quad \eta_i = \frac{\nu_i \tau}{\hbar},$$

$$\kappa = \frac{(\alpha')^2 \tau}{\hbar \cdot K} \rightarrow \kappa\omega^2 = \frac{\alpha' \cdot U \cdot \tau}{\hbar}, \qquad (4)$$

where $\hbar$ is the Planck's constant; Ω is dimensionless friction; κ is the key parameter of the coupling of the quantum subsystem to the classical one; and indices i of matrix elements ν and their dimensionless counterparts η correspond to 0, 1, X, 01, $0X$, and $1X$. In the dimensionless form, system (1) takes the form

$$ib_0 = \eta_{01}b_1 + \eta_{0X}b_X + \eta_0 b_0,$$
$$ib_1 = \eta_{1X}b_X + \eta_{01}b_0 + \kappa\omega^2,$$
$$ib_X = \eta_{1X}b_1 + \eta_{0X}b_0 + \kappa\omega^2 + \eta_X b_X, \qquad (5)$$
$$\ddot{u}_1 = -\omega^2 u_1 - \Omega\dot{u}_1 - |b_1|^2,$$
$$\ddot{u}_X = -\omega^2 u_X - \Omega\dot{u}_X - |b_X|^2.$$

System (5) was studied by varying five main parameters: η_0, η_1, η_X, ω_2, and κ. The first three parameters were varied randomly. The ω_2 value was varied in the range of 0.0005−0.003 as described above. For κ, integers from 4 to 46 were set. According to expressions (2) and (4), number 46 is the maximum κ value at which

the observed condition $\alpha' \leq 6.5$ eV Å^{-1} is observed for the selected lower boundary of the ω^2 range.

Numerical calculations were performed with the following initial conditions:

$$|b_1|^2 = 1, |b_0|^2 = |b_X|^2 = 0, u_1 = u_X = 0.$$

We found a number of combinations of parameters in which the behavior of the model was close to the experimental data. Figure 3 shows the population dynamics of states $S_{0\text{Rh}}$, $S_{1\text{Rh}}$, and $S_{0\text{Photo}}$ at the following parameter values: $\kappa = 9$, $\omega^2 = 0.00106$, $\eta_{1X} = 0.159$, $\eta_{0X} = 0.009$, and $\eta_{01} = 0.101$.

It should be noted that, at the given combination of parameters (as well as at some other combinations), the model quite accurately reproduces the behavior of photoexcited rhodopsin and is in good agreement with the published data. The calculated quantum yield is 0.67, which completely corresponds to the value obtained in experiments [4]. The evolution of the quantum subsystem is actually completed within 125 fs. This also coincides with the experimentally determined transition time of photoexcited chromophore from the PES level $S_{1\text{Rh}}$ to the ground energy level of the primary photoproduct $S_{0\text{Photo}}$ [2, 3]. The time to reach the conical intersection, determined in calculations, is approximately 30 fs, which actually coincides with the last assessment made by Johnson et al. [14] on the basis of recent experimental data obtained by laser-induced resonant gratings. Figure 3 clearly shows that two phases can be distinguished in the quantum subsystem evolution. In the first phase, a sharp increase in the population of the primary photoproduct $S_{0\text{Photo}}$ and a slight increase in the population of the initial rhodopsin state $S_{0\text{Rh}}$ are observed. In the second phase, the mean population $S_{0\text{Photo}}$ does not change, and the excited state $S_{1\text{Rh}}$ passes only to $S_{0\text{Rh}}$. This also agrees well with the assumption of the quantum transition coherence [2, 3, 14, 15]. Figure 4 shows the fluctuations of point masses of the classical sub-
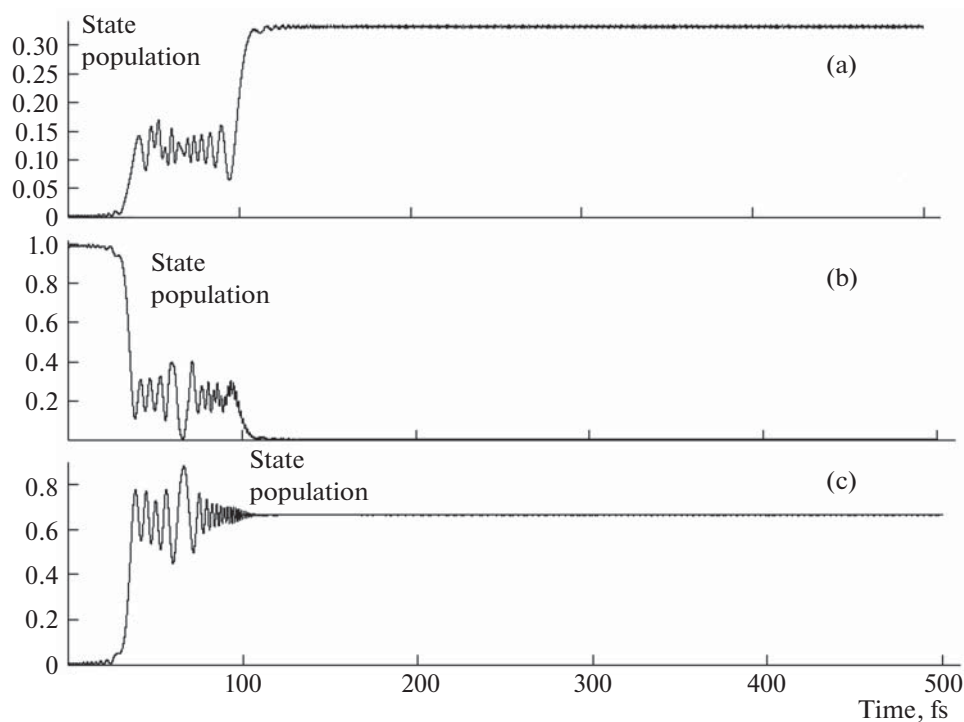
Fig. 3. The evolution of the population of different quantum states of the rhodopsin chromophore within the first 500 fs after its photoexcitation: (a) S_{0Rh}, (b) S_{1Rh}, and (c) S_{0Photo}.
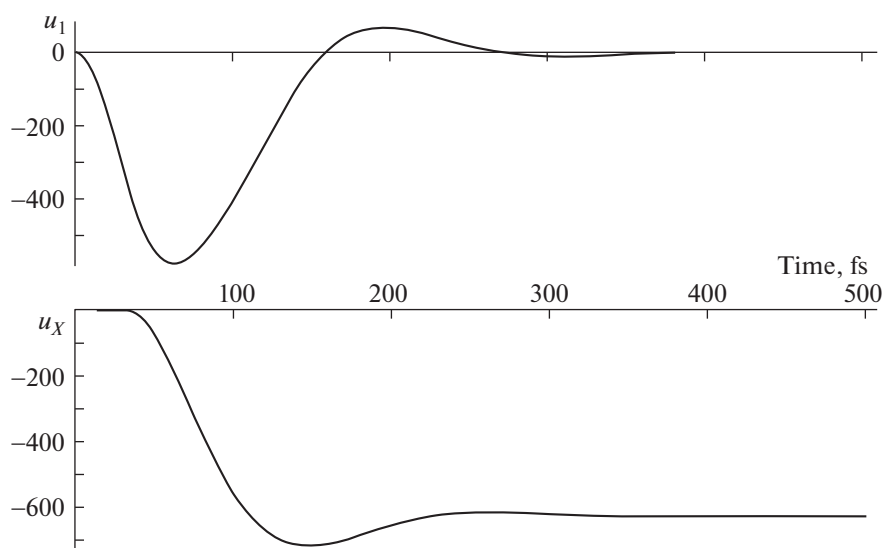
Fig. 4. The classical subsystem of the model during 11-*cis*-retinal photoisomerization: (a) measurement of the coordinate u_1 and (b) change in u_X. The stabilization of the second point mass in the new position, which corresponds to isomerization, is well seen in Fig. 4b.

system model. Their concordance and a clear correlation between the behavior of the classical and quantum subsystems are well seen. The period of fluctuations of atomic groups of the chromophore during its photoisomerization was approximately 226 fs. The corresponding frequency (147 cm^{-1}) perfectly agrees with the experimental frequencies of fluctuations of the molecular lattice of retinal involved in its photoisomerization: 136, 149, and 156 cm^{-1} [5, 14, 15]. According to our experiments, the specified reaction

frequencies for a wave packet that is observed in the dynamics of formation of the primary products of rhodopsin photoisomerization.

It is important to note that the best agreement between the calculated and experimental data was observed at the maximally realistic initial parameters of the model in terms of molecular biophysics. For example, $\omega^2 = 0.00106$ corresponds to the frequency of 1085 cm^{-1}, which is close to the range of common vibration frequencies of C−C and C−H bonds, equal to 1100−1300 cm^{-1} [13]. Figure 4 clearly shows that the characteristic shift of ne of the point masses is approximately 600 dimensionless units. It can be easily found from Eqs. (2) and (4) that, for $\kappa = 9$ and $\omega^2 = 0.00106$, this shift is approximately 0.9 Å, which is consistent with the notion of the local nature of molecular rearrangements of the chromophore at the initial stage of rhodopsin phototransformation. In this case, $\alpha' = 4.19$ eV Å^{-1}, i.e., well fits the allowable range.

Thus, the quantum−classical approach used in this study, despite its simplicity, makes it possible to reproduce many experimental data on the quantum yield of photoisomerization of 11-cis retinal in rhodopsin, its dynamics, and coherent nature. Therefore, there is every reason to conclude that the proposed model can be used to study the mechanism of ultrafast photoisomerization of retinal chromophore in the large family of retinal-containing proteins.

ACKNOWLEDGMENTS

SPELL: 1. ne

REFERENCES

1. Menon, S.T., Han, M., and Sakmar, T.P., *Physiol. Rev.*, 2001, vol. 81, pp. 1659−1688.
2. Nadtochenko, V.A., Smitienko, O.A., Feldman, T.B., Mozgovaya, M.N., Shelaev, I.V., Gostev, F.E., Sarkisov, O.M., and Osrovsky, M.A., *Dokl. Biochem. Biophys.*, 2012, vol. 446, pp. 242−246.
3. Polli, D., Altoe, P., Weingart, O., Spillane, K.M., Manzoni, C., Brida, D., Tomasello, G., Orlandi, G., Kukura, P., Mathies, R.A., Garavelli, M., and Cerullo, G., *Nature*, 2010, vol. 467, pp. 440−443.
4. Dartnall, H.J., *Vision Res.*, 1968, vol. 8, pp. 339−358.
5. Schoenlein, R.W., Peteanu, L.A., Mathies, R.A., and Shank, C.V., *Science*, 1991, vol. 254, pp. 412−415.
6. Andruniow, T., Ferre, N., and Olivucci, M., *Proc. Natl. Acad. Sci. U. S. A.*, 2004, vol. 101, pp. 17908−17913.
7. Isin, B., Schulten, K., Tajkhorshid, E., and Bahar, I., *Biophys. J.*, 2008, vol. 95, pp. 789−803.
8. Kholmurodov, Kh.T., Feldman, T.B., and Ostrovsky, M.A., *Mendeleev Communs.*, 2006, vol. 1, pp. 1−8.
9. Lakhno, V.D., *Phys. Chem. Chem. Phys.*, 2002, vol. 4, pp. 2246−2250.
10. Lakhno, V.D., *J. Biol. Phys.*, 2005, vol. 31, pp. 145−159.
11. Shigaev, A.S., Ponomarev, O.A., and Lakhno, V.D., *Chem. Phys. Lett.*, 2011, vol. 513, pp. 276−279.
12. Lemaitre, V., Yeagle, P., and Watts, A., *Biochemistry*, 2005, vol. 44, pp. 12667−12680.
13. Lin, S.W., Groesbeek, M., van der Hoef, I., Verdegem, P., Lugtenburg, J., and Mathies, R.A., *J. Phys. Chem. B*, vol. 102, pp. 2787−2806.
14. Johnson, P.J.M., Halpin, A., Morizumi, T., Prokhorenko, V.I., Ernst, O.P., and Miller, R.J.D., *Nat. Chem.*, 2015, vol. 7, pp. 980−986.
15. Smitienko, O.A., Mozgovaya, M.N., Shelaev, I.V., Gostev, F.E., Feldman, T.B., Nadtochenko, V.A., Sarkisov, O.M., and Ostrovsky, M.A., *Biochemistry* (Moscow), 2010, vol. 75, pp. 25−35.

Translated by M. Batrukova